



Cite this: *J. Mater. Chem. A*, 2024, **12**, 16729

Energetic multifunctionalized nitro/nitramino isomeric pyrazole–tetrazole hybrids: enhancing density and detonation properties through hydrogen bonding and π – π interactions[†]

Vikranth Thaltiri, ^a Richard J. Staples ^b and Jean'ne M. Shreeve ^{*a}

This study focuses on synthesizing high-density isomeric pyrazole–tetrazoles and their energetic salts, with a particular emphasis on improving detonation performance. First synthesized was 5-(3,4-dinitro-1*H*-pyrazol-5-yl)-1*H*-tetrazole ($\text{H}_2\text{DNP-5T}$, **3**), an isomer of 5-(3,4-dinitro-1*H*-pyrazol-4-yl)-1*H*-tetrazole ($\text{H}_2\text{DNP-4T}$) followed by synthesis of the nitramine derivative *N*-(4-nitro-5-(1*H*-tetrazol-5-yl)-1*H*-pyrazol-3-yl)nitramide ($\text{H}_3\text{NANP-5T}$, **11**) to further enhance detonation properties. Crystal packing and NCI analysis were used to gain insight into the impact of significant interactions such as hydrogen bonding and π – π interactions on density enhancement. Isomeric pyrazole–tetrazole ($\text{H}_2\text{DNP-5T}$) demonstrated high density and superior detonation properties compared to its 4-substituted derivative, $\text{H}_2\text{DNP-4T}$, attributed to increased inter-hydrogen bonding interactions, a high packing coefficient (73.1%), and π – π interactions. All substances were characterized spectroscopically using NMR, IR, and elemental analyses. The structures of compounds $\text{H}_2\text{DNP-5T}$, $\text{H}_3\text{NANP-5T}$, and **4** were further confirmed by single-crystal X-ray diffraction. Using EXPLO5 software, the detonation parameters of energetic materials based on experimental density and computed heat of formation were determined. Furthermore, the nitramine derivative $\text{H}_3\text{NANP-5T}$ (D_v : 8846 m s⁻¹; P : 33.2 GPa) and its energetic salts **13** (D_v : 9414 m s⁻¹; P : 34.5 GPa) and **14** (D_v : 9088 m s⁻¹; P : 33.9 GPa) exhibit outstanding detonation properties comparable to RDX. Comprehensive molecular and crystal-level insights into the impact of positional isomerism which hold significance for the design and development of new energetic materials.

Received 4th May 2024
Accepted 4th June 2024

DOI: 10.1039/d4ta03084b
rsc.li/materials-a

Introduction

Development of novel high energy density materials (HEDMs) for defense and space applications has been a fascinating and challenging pursuit for synthetic chemists globally.^{1,2} The nitro group has played a vital role in the advancement of energetic materials (EMs). Traditional energetic polynitro compounds such as, 2,4,6,8,10,12-hexanitro-2,4,6,8,10,12-hexaazatetracyclododecane (CL-20), 1,3,5-trinitro-1,3,5-triazacyclo-hexane (RDX), 2,4,6-trinitrotoluene (TNT), and 1,3,5,7-tetranitro-1,3,5,7-tetra-azacyclooctane (HMX) derive energy from the oxidation of carbon and hydrogen frameworks upon detonation.^{3,4} Incorporating more nitro groups into a structure enhances detonation performance but has synthetic challenges and raises environmental concerns. These include increased hazardous byproduct generation, waste

management complexities, generation of acid wastes, and difficulties in handling strong oxidizing and hygroscopic reagents such as fuming HNO_3 or 100% HNO_3 . Excess nitro groups may compromise structural stability, leading to increased sensitivity and reduced thermal stability.^{5,6} Hence, developing environmentally friendly and insensitive EMs requires dedicated research efforts. Modern heterocyclic energetic compounds derive their energy not only from the oxidation of the backbone but also from high nitrogen content.^{5,6} EMs with high nitrogen content not only contribute to higher heats of formation, but predominantly yield environmentally benign molecular nitrogen as a byproduct of detonation.^{7,8} Among the notable family of innovative high energy density materials are azole-based compounds, prized for their typically high endothermic nature, dense composition, low sensitivity to external stimuli, and high detonation properties. Numerous investigators have explored the combination of these homo/hetero azoles, resulting in a plethora of compounds exhibiting remarkable detonation properties as energetic materials.

The advance of isomer chemistry in the field of energetic materials not only broadens research approaches, but also takes precedent from pioneering innovations in synthetic pharmaceutical chemistry. This emerging topic has received

^aDepartment of Chemistry, University of Idaho, Moscow, Idaho, 83844-2343, USA.
E-mail: jshreeve@uidaho.edu

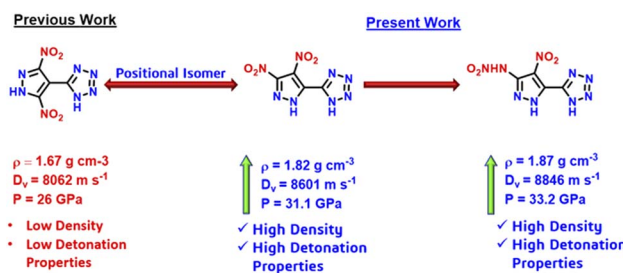
^bDepartment of Chemistry, Michigan State University, East Lansing, Michigan 48824, USA

[†] Electronic supplementary information (ESI) available. CCDC 2352179, 2352182 and 2352182. For ESI and crystallographic data in CIF or other electronic format see DOI: <https://doi.org/10.1039/d4ta03084b>



considerable attention, highlighting the importance of isomer chemistry in advancing the research and development of energetic materials. Variations in molecular structure due to positional isomerism influence properties such as stability, density, sensitivity, and so on profoundly.^{9–15} The concept of designing hybrid heterocycles offers significant advantages in tailoring the energetic properties of compounds. This approach not only allows for the optimization of specific properties but also provides opportunities to obtain compounds with new properties with a wider range of practical applications.^{16–18} In recent years, researchers have explored the combination of tetrazole with various other heterocycles.^{19–21} The C–C linkage between these heterocycles takes advantage of the energetic tetrazole ring, the enhanced stability of the 1*H*-1,2,4-triazole/2*H*-1,2,3-triazole, and the presence of various energetic groups on the second carbon atom of the triazole (Scheme 1).^{22–24} To further enhance the energetic performance, utilizing a pyrazole molecule rather than a triazole is another option. Pyrazoles have relatively high heats of formation, exhibit high thermal stability and provide a position for an additional nitro group due to the presence of three carbon atoms.²⁵ The importance of hydrogen bonds and π – π interactions in the construction of energetic materials stems from their advantageous impact on both physical and chemical properties. A promising approach to developing HEDMs is to strategically introduce energetic groups as proton acceptors, which can result in strong hydrogen bond formation. Increased intra- and intermolecular interactions within the molecule can give rise to more compact packing, which leads to smaller volumes thus leading to improved stability and density of these materials. Nitramino-based compounds and their energetic salts exhibit advantageous energetic characteristics due to their high heats of formation and good chemical composition. The nitramino group, composed of amino and nitro groups, serves as both a hydrogen donor and acceptor, enabling successive hydrogen bonding interactions.²⁶

Benz reported the first example of a fully nitro-functionalized pyrazole–tetrazole hybrid, 5-(3,5-dinitro-1*H*-pyrazol-4-yl)-1*H*-tetrazole (**H₂DNP-4T**), and its energetic derivatives.²⁷ However,



Scheme 2 Comparison of C–C bridged isomeric pyrazole–tetrazole hybrids.

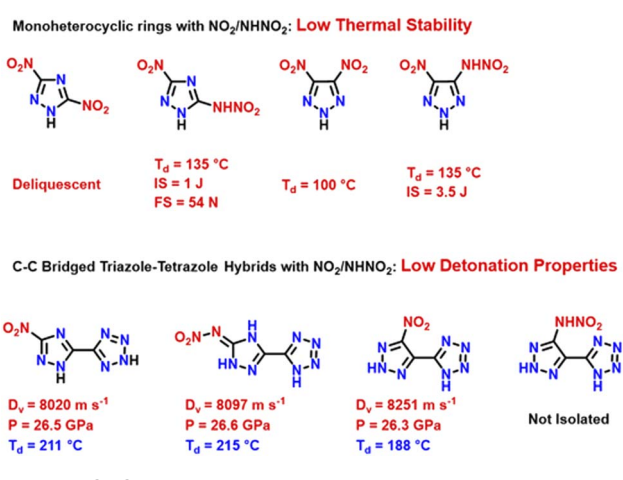
compound **H₂DNP-4T** exhibits low detonation performance (D_v : 8062 m s⁻¹; P : 26 GPa) because of its low density of 1.669 g cm⁻³, which results from the non-coplanarity of both rings (Scheme 2). Achieving a density > 1.80 g cm⁻³ is imperative for the fabrication of advanced EMs, as it is directly contributing to the high detonation performance. Therefore, we endeavoured to implement our proposed approaches in designing a higher density isomer of the pyrazole–tetrazole hybrid.

In this study, we have synthesized successfully highly dense isomeric pyrazole–tetrazoles which contain energetic substituents such as nitro/nitramino groups, along with their corresponding energetic salts. This research focuses on investigating the influence of positional isomers and the presence of energetic moieties on the structural and energetic properties of these compounds. Concomitantly the potential application of the synthesized compounds as energetic materials is assessed by analyzing experimentally obtained values of thermal decomposition, sensitivity data, and calculated detonation properties. This comprehensive study provides valuable insights into the design and evaluation of novel energetic materials.

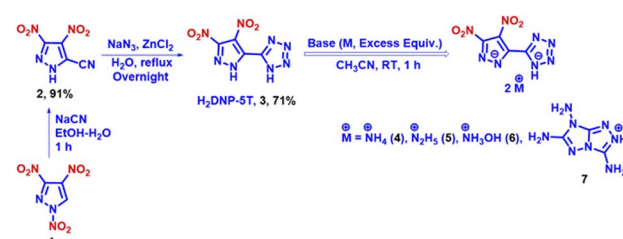
Results and discussion

Synthesis

The synthesis of 5-(3,4-dinitro-1*H*-pyrazol-5-yl)-1*H*-tetrazole (**H₂DNP-5T**, **3**) commences with the modified cyanation of 1,3,4-trinitropyrazole using sodium cyanide to give an excellent yield. Subsequently, the [3 + 2] cycloaddition reaction with NaN₃, catalyzed by ZnCl₂, gave **H₂DNP-5T** in 71% yield. The corresponding energetic salts (**4**, **5**, **6**, and **7**) of **H₂DNP-5T** were synthesized by diluting the neutral compound in acetonitrile with subsequent addition of the corresponding base (Scheme 3)

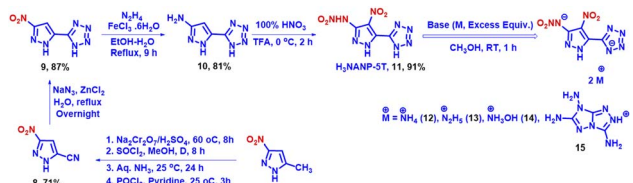


Scheme 1 C–C bridged triazole–tetrazole hybrids.

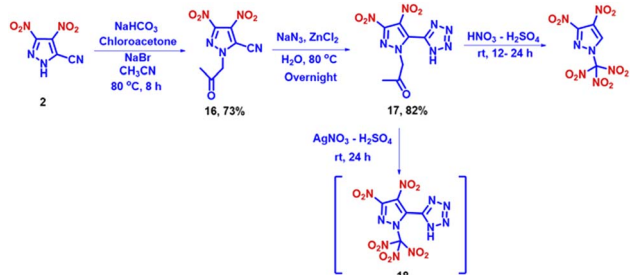


Scheme 3 Synthesis of **H₂DNP-5T** (**3**) and its ionic derivatives, **4**, **5**, **6**, and **7**.





Scheme 4 Synthesis of compound $\text{H}_3\text{NAP-5T}$ (11) and its ionic derivatives 12, 13, 14, and 15.



Scheme 5 Synthetic scheme for compound 18.

at room temperature. The corresponding salts precipitated quickly and in very good yields. The nitramine derivative of $\text{H}_3\text{NAP-5T}$ (11) was prepared with an alternate synthetic route to Dalinger (from a low overall yield of 3-cyanopyrazole) from 3-nitro-5-cyanopyrazole (8), which was synthesized from 3-nitro-5-methylpyrazole (detailed scheme in ESI, Scheme S2†).²⁸ The [3 + 2] cycloaddition follows a similar procedure to that of in compound 9. The catalytic reduction of the nitro group was conducted using hydrazine in the presence of an Fe(III)salt. Nitration of compound 10 with the mild nitrating reagent $\text{HNO}_3\text{-CF}_3\text{COOH}$, led to the formation of the desired target, $\text{H}_3\text{NAP-5T}$, in excellent yield (Scheme 4). The nitrogen-rich energetic salts of the latter were synthesized by the addition of an excess of the corresponding base in methanol at room temperature. The salts containing two monovalent cations per anion precipitated in the reaction mixture, while no salts with three cations per anion were observed even at elevated temperatures. In addition, we have sought to introduce the *N*-trinitromethyl group into compound 3 (Scheme 5). The *N*-acetylation of the sodium salt derivative of 2 prepared *in situ* with chloroacetone in the presence of NaBr resulted in the formation of 16. Compound 17 was prepared successfully in a similar procedure with Na_3N and ZnCl_2 . Subsequently, treatment with a mixed acid nitrating mixture ($\text{HNO}_3\text{-H}_2\text{SO}_4$), facilitated tetrazole cleaved 3,4-dinitro-1-(trinitromethyl)-1*H*-pyrazole, which was confirmed through NMR analysis. Despite attempts at nitration with various metal nitrates (KNO_3 , NaNO_3 , NHNO_3 , and AgNO_3) and sulfuric acid, product formation was only observed using $\text{AgNO}_3\text{-H}_2\text{SO}_4$. Regrettably, the intended product (18) could not be purified or be thoroughly characterized due to its precipitation in conjunction with silver sulfate. However, the product (18) was confirmed by NMR (^1H , ^{13}C , and ^{14}N ; ESI (Fig. S46–S48†)) and HRMS spectroscopy (ESI,

Fig. S49†). All the newly synthesized compounds were characterized spectroscopically by NMR (^1H , ^{13}C , and ^{14}N), IR and elemental analysis.

Single crystal structure analysis

Suitable single crystals of $\text{H}_2\text{DNP-5T}$, $\text{H}_2\text{NAP-5T-DMA}$ (11-DMA), and 4 were obtained for SC-XRD analysis through slow evaporation of acetonitrile-methanol, DMF-AcOH, and water-methanol solutions, respectively. The crystallographic information is available in the (ESI†). $\text{H}_3\text{NAP-5T}$ undergoes crystallization in various solvents culminating in successful crystallization with dimethyl amine in a dimethylformamide-acetic acid solvent system. The crystal structure of $\text{H}_2\text{DNP-5T}$, was determined in the monoclinic space group $P2_1/n$ with a cell volume 813.238 \AA^3 , having one formula unit in the asymmetric unit. Notably, it exhibits a crystal density of 1.847 g cm^{-3} at 100 K , which is higher than that of the 4-substituted derivative ($\text{H}_2\text{DNPT-4T}$). The torsion angles of $\text{N}2\text{-N}1\text{-C}1\text{-C}2$ and $\text{N}4\text{-N}3\text{-C}4\text{-N}6$ are 0.33° and -0.23° , indicating that each pyrazole and tetrazole ring has a planar structure. However, both rings are not completely planar with each other ($\text{N}3\text{-C}4\text{-C}1\text{-N}1 - 142.7^\circ$) (Fig. 1). Additionally, it shows two inter molecular hydrogen bonds, $\text{N}1\text{-H}1\cdots\text{N}6$ and $\text{N}3\text{-H}3\cdots\text{N}2$ with a distance of 1.96 and 2.06 \AA respectively.

The structure of 11-DMA is in the triclinic space group $P\bar{1}$ with a cell volume of 558.18 \AA^3 , with a single unit within the cell. It has a calculated crystal density of 1.703 g cm^{-3} . The torsion angles of $\text{C}2\text{-C}3\text{-C}4\text{-N}6$ (-177.8°) and $\text{N}2\text{-C}3\text{-C}4\text{-N}3$ (178.7°) support coplanarity of both rings. The nitro groups are also planar ($\text{O}3\text{-N}9\text{-C}2\text{-C}1$ 175.5° and $\text{O}1\text{-N}8\text{-N}7\text{-N}1$ -4.36°) with the pyrazole moiety. The nitramine group forms extended intramolecular hydrogen bonds ($\text{N}3\text{-H}3\cdots\text{O}3$ 2.048 \AA and $\text{N}1\text{-H}1\cdots\text{O}1$ 2.072 \AA). This configuration results in a face-face molecular arrangement with an inter-layer distance of 3.351 \AA , facilitating potential $\pi\text{-}\pi$ stacking interactions within the crystal, thereby contributing to molecular stability. The structure of compound 4 was elucidated in the $P2_1/n$ space group, with a single unit in the cell with a calculated crystal density of 1.712 g cm^{-3} at 100 K .

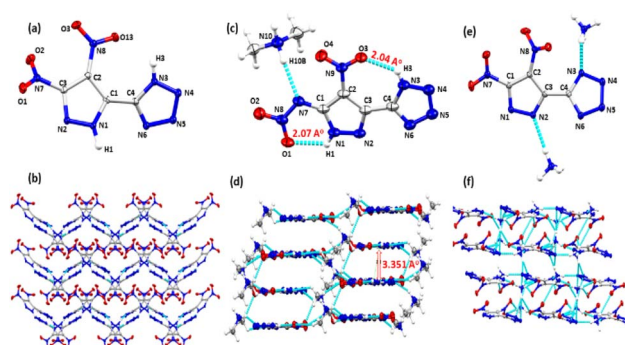


Fig. 1 (a) Thermal ellipsoid plot (50%) of $\text{H}_2\text{DNP-5T}$ (3). (b) Packing and H-bonding in compound $\text{H}_2\text{DNP-5T}$. (c) Thermal ellipsoid plot (50%) of 11-DMA. (d) Packing and H-bonding in 11-DMA. (e) Thermal ellipsoid plot (50%) of 4. (f) Packing and H-bonding in compound 4.



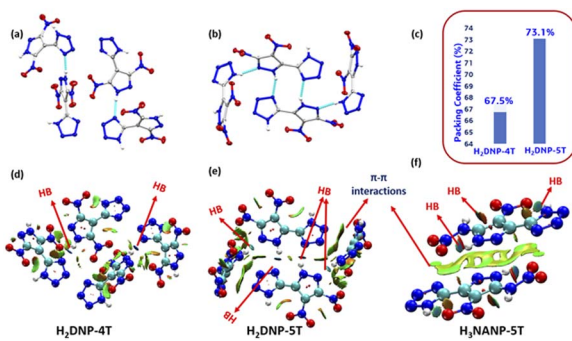


Fig. 2 (a) Hydrogen bond interactions in **H**₂DNP-4T; (b) hydrogen bond interactions in **H**₂DNP-5T; (c) comparison of packing coefficient of **H**₂DNP-4T and **H**₂DNP-5T; (d)–(f) noncovalent interaction plots of gradient isosurfaces **H**₂DNP-4T, **H**₂DNP-5T, and **H**₃NANP-5T, respectively.

Density of energetic materials – NCI analysis

Density is a pivotal parameter in the assessment of EMs, directly influencing detonation performance since the detonation velocity and detonation pressure are proportional to density. The densities of **H**₂DNP-5T, **H**₃NANP-5T, and their salts were measured using a gas pycnometer at 25 °C, to give measured densities of 1.82 g cm⁻³ and 1.872 g cm⁻³ for **H**₂DNP-5T and **H**₃NANP-5T, respectively. Molecular packing dictates the density of EMs, as demonstrated by the arrangement of pyrazole and tetrazole rings in **H**₂DNP-5T fostering more inter-molecular hydrogen bonds between the acidic protons and the nitrogen atoms of the pyrazole and the tetrazole moieties (Fig. 2(b)) and thereby achieving closer packing than in **H**₂DNP-4T, which exhibits hydrogen bonds between the acidic proton and the nitrogen atoms of tetrazole only (Fig. 2(a)). As a result, **H**₂DNP-5T exhibits a higher packing coefficient of 73.1% and consequently, a higher density (Fig. 2(c)). Further insights into inter- and intramolecular interactions were gained through Non-Covalent Interactions (NCI) using Multiwfn software with the

resulting plots being analyzed using VMD software (Fig. 2).^{29,30} The analysis revealed abundant NCI domains in **H**₂DNP-5T compared to **H**₂DNP-4T attributed to π-π interactions, contributing to the higher density. **H**₃NANP-5T exhibited much stronger face-to-face interactions, further enhancing its density. Overall, the densities of **H**₂DNP-5T and **H**₃NANP-5T are attributed to their regular close packing with packing coefficient of 73.1%, hydrogen bonding, and π-π interactions, as supported by experimental observation and theoretical analysis. Ionic derivatives of **H**₂DNP-5T and **H**₃NANP-5T have densities in the range between 1.69 and 1.77 g cm⁻³ and 1.77–1.83 g cm⁻³ respectively, with the hydrazinium salt derivatives exhibiting the highest density of 1.78 g cm⁻³ for 5 and 1.83 g cm⁻³ for 13.

Thermal behavior, detonation properties, and sensitivity

Since all compounds are EMs, their energetic properties were thoroughly examined. In Table 1, the theoretically calculated and experimentally determined physicochemical values, juxtaposed with the data for RDX to allow comparative analysis. Knowing the thermal stability is vital for synthesizing physically stable EMs. Differential scanning calorimetry (DSC) was used to determine the thermal behavior of all the compounds at a heating rate of 5 °C min⁻¹. Among all the compounds examined, TATOT energetic salts displayed the highest decomposition temperatures of 212 °C (7) and 221 °C (15). **H**₂DNP-5T exhibited an onset decomposition temperature of 193 °C, nearly identical to its isomer, **H**₂DNP-4T. The nitramine derivative, **H**₃NANP-5T, demonstrated a decomposition temperature of 165 °C, suitable for applications in energetic materials. Ionic derivatives of **H**₂DNP-5T showed decomposition temperatures ranging from 131 °C to 212 °C. Notably, the energetic salts (12–15) of the nitramine derivative (11) exhibited significantly higher decomposition temperatures, ranging from 183 °C to 221 °C, compared to the derivatives of **H**₂DNP-5T, which can be attributed to hydrogen bonding interactions and face-face stacking. The hydrazinium (5) and hydroxylammonium (6) salts of **H**₂DNP-5T displayed poor thermal stability, with

Table 1 Physicochemical and energetic properties^k

Compound	ρ^a (g cm ⁻³)	D_v^b (m s ⁻¹)	P^c (GPa)	T_d^d (°C)	ΔH_f^e (kJ mol ⁻¹)	IS^f (J)	FS^g (N)
3	1.82 (1.847) ^h	8601	31.1	193	521	8	160
4	1.69 (1.712) ^h	8139	24.9	196	313	16	360
5	1.78	9017	31.3	139	633	15	240
6	1.73	8687	30.9	131	444	14	240
7	1.77	8431	30.9	212	1556	25	360
11	1.872	8846	33.2	165	552	12	160
12	1.766	8570	27.7	210	302	20	360
13	1.83	9414	34.5	183	623	16	360
14	1.825	9088	33.9	187	427	14	360
15	1.817	8723	28.7	221	1539	30	360
H ₂ DNP-4T ⁱ	1.669	8062	26.0	207	517.1	2.0	120
RDX ^j	1.80	8795	34.9	204	92.6	7.4	120

^a Density determined by gas pycnometer at 25 °C. ^b Detonation velocity. ^c Detonation pressure. ^d Thermal decomposition temperature (5 °C min⁻¹).

^e Heat of formation. ^f Impact sensitivity (BAM drophammer). ^g Friction sensitivity (BAM friction tester). ^h Crystal density at 100 K. ⁱ Ref. 27. ^j Ref. 33.

^k Note 1: densities used for EXPLO calculations were measured values obtained via pycnometry; note 2: the IS and FS values were obtained using powder samples.



decomposition temperatures of 139 °C and 131 °C, respectively. Using the isodesmic reaction approach, the heats of formation (HoF) of all EMs were calculated by using Gaussian09.³¹ High positive heats of formation (ΔH_f) ranging from 302 to 1556 kJ mol⁻¹ were observed for all compounds, primarily attributed to the tetrazole ring. Notably, the TATOT salts of **H₂DNP-5T** (3) and **H₃NANP-5T** (11) exhibited the highest heats of formation at 1539 kJ mol⁻¹ and 1556 kJ mol⁻¹, respectively, due to the contribution from the TATOT cation.

Using EXPLO5 software (version 7.01.01), detonation properties including velocity of detonation (D_v) and detonation pressure (P) were computed based on the calculated heats of formation and measured densities by pycnometer.³² The calculated detonation velocities range from 8139 (4) to 9414 m s⁻¹ (13), with corresponding detonation pressures between 24.9 (4) and 34.5 GPa (13). Significantly, the 5-substituted isomer **H₂DNP-5T**, demonstrated superior detonation properties (D_v : 8601 m s⁻¹; P : 31.1 GPa), outperforming its 4-substituted derivative and approaching those of RDX, owing to its high density (1.82 g cm⁻³). The neutral nitramine derivative **H₃NANP-5T** displayed excellent detonation properties comparable to RDX (D_v : 8795 m s⁻¹; P : 34.9 GPa), with D_v : 8846 m s⁻¹ and P : 33.2 GPa. Remarkably, the hydrazinium (13) and hydroxylammonium (14) salts of the nitramine derivative (11) exhibited higher detonation properties among all compounds (D_v : 9414 m s⁻¹; P : 34.5 GPa for compound 13; D_v : 9088 m s⁻¹; P : 33.9 GPa for compound 14) with good thermal stabilities of 183 °C and 187 °C, respectively.

Using BAM technology, the impact and friction sensitivities of all the compounds were determined (Table 1). The neutral nitramine derivative **H₃NANP-5T** displayed lower sensitivity (IS: 12 J) compared to the neutral nitro derivative **H₂DNP-5T** (IS: 8 J), potentially attributed to strong π – π stacking and hydrogen bonding interactions. Ionic derivatives exhibited insensitivity towards friction (240–360 N) and acceptable impact sensitivity (14–30 J) due to larger N···H and O···H interactions (Fig. 3, Hirshfeld surface analysis). TATOT derivatives displayed improved impact values (25 J for 7 and 30 J for 15). Importantly,

all the compounds exhibited lower sensitivities than the commonly used secondary energetic material, RDX. Furthermore, the ionic derivatives (12–15) of **H₃NANP-5T**, displayed superior impact and friction values compared to the ionic derivatives (4–7) of **H₂DNP-5T**.

Conclusions

We have successfully designed and synthesized the high-density isomeric pyrazole–tetrazole hybrid, **H₂DNP-5T** (3) and further enhanced its detonation properties by synthesizing the nitramine derivative, **H₃NANP-5T**. The high-density observed in both the compounds is primarily attributed to the molecular arrangement of pyrazole and tetrazole rings, which foster intra-inter-molecular hydrogen bonds, a high packing coefficient, and π – π interactions. Notably, **H₃NANP-5T** exhibited excellent detonation properties (D_v : 8846 m s⁻¹; P : 33.2 GPa), comparable to RDX, along with satisfactory thermal stability (165 °C) and sensitivity (IS: 12 J; FS: 160 N), making it a promising candidate for application as an energetic material. The ionic derivatives displayed enhanced stabilities and excellent detonation properties, exemplified by 5 (D_v : 9017 m s⁻¹; P : 31.3 GPa; IS: 15 J; FS: 240 N), 6 (D_v : 8687 m s⁻¹; P : 30.9 GPa; IS: 14 J; FS: 240 N), 13 (D_v : 9414 m s⁻¹; P : 34.5 GPa; IS: 16 J; FS: 360 N), and 14 (D_v : 9088 m s⁻¹; P : 33.9 GPa; IS: 14 J; FS: 360 N). This work highlights the significance of positional isomerism and the presence of energetic moieties (nitro/nitramino) in influencing both structural and energetic properties.

Data availability

All data supporting findings of this study are available within the article and its ESI.†

Author contributions

V. T. investigation, methodology, conceptualization and manuscript writing. R. J. S. X-ray data collection and structures solving. V. T. and J. M. S. conceptualization, manuscript writing-review and editing, supervision.

Conflicts of interest

There are no conflicts to declare.

Acknowledgements

The Rigaku Synergy S Diffractometer was purchased with support from the National Science Foundation MRI program (1919565). We are grateful for the support of the Fluorine-19 fund.

References

- 1 J. P. Agrawal, *High Energy Materials: Propellants, Explosives and Pyrotechnics*, Wiley-VCH, Weinheim, 2010.

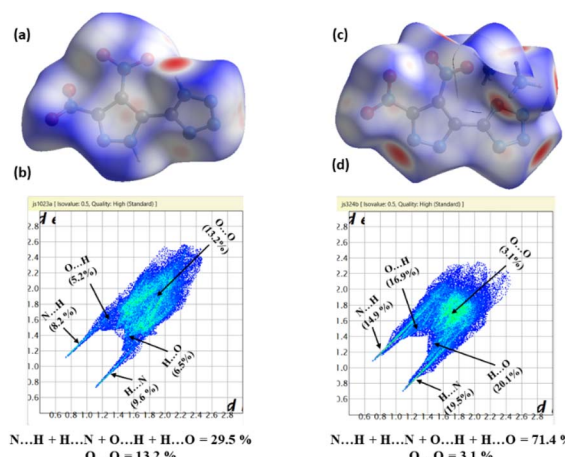


Fig. 3 Hirshfeld surface graphs and 2D fingerprint plots of **H₂DNP-5T** (3) and 4 (c and d).



2 T. M. Klapötke, *Chemistry of High-Energy Materials*, de Gruyter, Berlin, 6th edn, 2022.

3 D. M. Badgujar, M. B. Talawar, S. N. Asthana and P. P. Mahulikar, *J. Hazard. Mater.*, 2008, **151**, 289.

4 V. Thaltiri, K. Chavva, B. S. Kumar and P. K. Panda, *New J. Chem.*, 2019, **43**, 12318.

5 G. Hervé, C. Roussel and H. Graindorge, *Angew. Chem., Int. Ed.*, 2010, **49**, 3177.

6 J. Singh, R. J. Staples and J. M. Shreeve, *Sci. Adv.*, 2023, **9**(46), eadk3754.

7 P. Yin and J. M. Shreeve, *Adv. Heterocycl. Chem.*, 2017, **121**, 89.

8 H. Gao and J. M. Shreeve, *Chem. Rev.*, 2011, **111**, 7377.

9 V. Thaltiri, J. Singh, R. J. Staples and J. M. Shreeve, *J. Mater. Chem. A*, 2024, **12**, 9546.

10 F. Chen, Y. Wang, S. Song, K. Wang and Q. Zhang, *J. Phys. Chem. C*, 2023, **127**, 8887.

11 L. M. Barton, J. T. Edwards, E. C. Johnson, E. J. Bukowski, R. C. Sausa, E. F. Byrd, J. A. Orlicki, J. J. Sabatini and P. S. Baran, *J. Am. Chem. Soc.*, 2019, **141**, 12531.

12 D. R. Wozniak, B. Salfer, M. Zeller, E. F. C. Byrd and D. G. Piercey, *Org. Lett.*, 2020, **22**, 9114.

13 Q. Sun, Z. Jiang, N. Ding, C. Zhao, B. Tian, S. Li and S. Pang, *J. Mater. Chem. A*, 2023, **11**, 23228.

14 Q. Sun, N. Ding, C. Zhao, J. Ji, S. Li and S. Pang, *Chem. Eng. J.*, 2022, **427**, 130912.

15 S. Liao, T. Liu, Z. Zhou, K. Wang, S. Song and Q. Zhang, *Dalton Trans.*, 2021, **50**, 13286.

16 M. Balaraju, N. Kommu, S. Vangara, A. K. Sahoo, V. Thaltiri and A. K. Sahoo, *Chem. Commun.*, 2024, **60**, 827.

17 (a) I. L. Dalinger, A. V. Kormanov, K. Yu. Suponitsky, N. V. Muravyev and A. B. Sheremetev, *Chem.-Asian J.*, 2018, **13**, 1165; (b) J. Tang, H. Xiong, Y. Tang, H. Yang and G. Cheng, *Dalton Trans.*, 2023, **52**, 3169; (c) J. Cai, C. Xie, J. Xiong, J. Zhang, P. Yin and S. Pang, *Chem. Eng. J.*, 2022, **433**, 134480.

18 Q. Ma, G. Zhang, J. Li, Z. Zhang, H. Lu, L. Liao, G. Fan and F. Nie, *Chem. Eng. J.*, 2020, **379**, 122331.

19 B. Chen, H. Lu, J. Chen, Z. Chen, S.-F. Yin, L. Peng and R. Qiu, *Top. Curr. Chem.*, 2023, **381**, 25.

20 S. Manzoor, Q. Tariq, X. Yin and J. G. Zhang, *Def. Technol.*, 2021, **17**, 1995.

21 P. Bhatia, K. Pandey, B. Avasthi, P. Das, V. D. Ghule and D. Kumar, *J. Org. Chem.*, 2023, **88**, 15085.

22 A. A. Dippold and T. M. Klapötke, *Chem.-Asian J.*, 2013, **8**, 1463.

23 D. Izsak, T. M. Klapötke and C. Pfluger, *Dalton Trans.*, 2015, **44**, 17054.

24 Y. Tang, Y. Liu, G. H. Imler, D. A. Parrish and J. M. Shreeve, *Org. Lett.*, 2019, **21**, 2610.

25 S. Zhang, Z. Gao, D. Lan, Q. Jia, N. Liu, J. Zhang and K. Kou, *Molecules*, 2020, **25**, 3475.

26 P. Yin, D. A. Parrish and J. M. Shreeve, *J. Am. Chem. Soc.*, 2015, **137**, 4778.

27 M. Benz, T. M. Klapötke and J. Stierstorfer, *Z. Anorg. Allg. Chem.*, 2020, **646**, 1380.

28 I. L. Dalinger, A. V. Kormanov, I. A. Vatsadze, O. V. Serushkina, T. K. Shkineva, K. Yu. Suponitsky, A. N. Pivkina and A. B. Sheremetev, *Chem. Heterocycl. Compd.*, 2016, **52**, 1025.

29 E. R. Johnson, S. Keinan, P. Mori-Sánchez, J. Contreras-García, A. J. Cohen and W. Yang, *J. Am. Chem. Soc.*, 2010, **132**, 6498.

30 T. Lu and F. Chen, *J. Comput. Chem.*, 2012, **33**, 580.

31 M. J. Frisch, G. W. Trucks, H. B. Schlegel, G. E. Scuseria, M. A. Robb, J. R. Cheeseman, G. Scalmani, V. Barone, G. A. Petersson, H. Nakatsuji, X. Li, M. Caricato, A. Marenich, J. Bloino, B. G. Janesko, R. Gomperts, B. Mennucci, H. P. Hratchian, J. V. Ortiz, A. F. Izmaylov, J. L. Sonnenberg, D. Williams-Young, F. Ding, F. Lipparini, F. Egidi, J. Goings, B. Peng, A. Petrone, T. Henderson, D. Ranasinghe, V. G. Zakrzewski, J. Gao, N. Rega, G. Zheng, W. Liang, M. Hada, M. Ehara, K. Toyota, R. Fukuda, J. Hasegawa, M. Ishida, T. Nakajima, Y. Honda, O. Kitao, H. Nakai, T. Vreven, K. Throssell, J. A. Montgomery Jr., J. E. Peralta, F. Ogliaro, M. Bearpark, J. J. Heyd, E. Brothers, K. N. Kudin, V. N. Staroverov, T. Keith, R. Kobayashi, J. Normand, K. Raghavachari, A. Rendell, J. C. Burant, S. S. Iyengar, J. Tomasi, M. Cossi, J. M. Millam, M. Klene, C. Adamo, R. Cammi, J. W. Ochterski, R. L. Martin, K. Morokuma, O. Farkas, J. B. Foresman and D. J. Fox, *Gaussian 09, Revision E.01*, Gaussian, Inc., Wallingford, CT, 2013.

32 M. Suceska, *EXPLO5 7.01.01*, Brodarski Institute, Zagreb, Croatia, 2013.

33 V. Thaltiri, V. Shanmugapriya, T. Yadagiri and P. K. Panda, *Asian J. Org. Chem.*, 2022, **11**, e202200487.

